Original Research Article

Physicochemical characterization, the Hirshfeld surface, and biological evaluation of two meloxicam compounding pharmacy samples

Luciana F.A. Romani [a], Maria I. Yoshida [a], Elionai C.L. Gomes [a], Renes R. Machado [b], Felipe F. Rodrigues [b], Márcio M. Coelho [b], Marcelo A. Oliveira [c], Maria B. Freitas-Marques [a], Rosane A.S. San Gil [d], Wagner N. Mussel [a,*]

[a] Department of Chemistry, Institute of Exact Sciences, Federal University of Minas Gerais, Av. Antônio Carlos 6627, Belo Horizonte, MG, Brazil
[b] Department of Pharmaceutical Products, Faculty of Pharmacy, Federal University of Minas Gerais, Av. Antônio Carlos 6627, Belo Horizonte, MG, Brazil
[c] Health Science Department, Federal University of Espírito Santo, Campus São Mateus, ES, Brazil
[d] Institute of Chemistry, Federal University of Rio de Janeiro, Campus Fundão, RJ, Brazil

A B S T R A C T

Meloxicam (MLX) is an anti-inflammatory drug susceptible to variations and crystalline transitions. In compounding pharmacies, the complete crystallographic evaluation of the raw material is not a routine procedure. We performed a complete crystallographic characterization of aleatory raw MLX samples from compounding pharmacies. X-ray diffraction indicated the presence of two crystalline forms in one sample. DSC experiments suggested that crystallization, or a crystal transition, occurred differently between samples. The FTIR and ^1H NMR spectra showed characteristic assignments. ^{13}C solid-state NMR spectroscopy indicated the presence of more than one phase in a sample from pharmacy B. The Hirshfeld surface analysis, with electrostatic potential projection, allowed complete assignment of the UV spectra in ethanol solution. The polymorph I of meloxicam was more active than polymorph III in an experimental model of acute inflammation in mice. Our results highlighted the need for complete crystallographic characterization and the separation of freely used raw materials in compounding pharmacies, as a routine procedure, to ensure the desired dose/effect.

1. Introduction

Meloxicam (MLX, Fig. 1), a non-steroidal anti-inflammatory drug (NSAID) and a partially selective cyclooxygenase (COX-2) inhibitor, belongs to the class of enolic acids and is derived from oxicam. Owing to its anti-inflammatory and analgesic effects as well as good safety profile, characterized by a low incidence of gastrointestinal side effects [1], it is widely prescribed. MLX, [4-hydroxy-2-methyl-N-(5-methyl-2-thiaolyl)−2H-1, 2- benzothiazine-3-carboxamide 1,1-dioxide] ($C_{14}H_{13}N_3O_4S_2$; 351.40 g mol^{-1}), is a yellow powder, practically insoluble in water, and slightly soluble in organic solvents, and well soluble in strong acids and bases [2,3].

In 2003, Coppi, Sanmarti, and Clavo [4] described five crystalline forms of MLX associated with the corresponding processes for preparation and interconversion. The forms have distinct network structures that may differ in biopharmaceutical aspects and compromise their own functions. Luger and colleagues [5] described the crystalline form I as the most suitable for the preparation of pharmaceutical products. The interconversion between different polymorphs may occur during the storage, as a consequence of the synthetic route, or in improper storage conditions with variations in humidity and temperature. As raw pharmaceutical materials are susceptible to variations and transitions, their full crystallographic analysis is important and should be adopted as a routine practice for adequate quality control. Only proper control will ensure the efficacy and safety of public health [6–10].

In the present study, we characterized and evaluated the biological activity of meloxicam raw material that is freely used in compounding pharmacies.

2. Experimental

MLX samples were obtained from three compounding pharmacies, and anonymized as A, B, and C, which corresponded to different routine batches of Indian origin: TDM/ML/002/11/12–13, ALC/MLX/120102, and MLAH16081112#5, respectively.
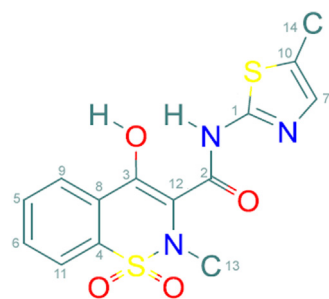
Fig. 1. The chemical structure of meloxicam.

2.1. Powder X-ray diffraction (PXRD)

PXRD data were collected by a XRD-7000 diffractometer (Shimadzu) at 22 °C at 40 kV and 30 mA, using $CuK_\alpha (\lambda = 1.54056 Å)$ equipped with a polycapillary focusing optics under parallel geometry coupled with a graphite monochromator. The sample was subjected to spinning at 60 rpm, scanned over an angular range of 4 60° (2θ) with a step size of 0.01° (2θ) and a time constant of 2 s/ step. The software CrystalExplorer v 3.1 was used for the Hirshfeld surface analysis.

2.2. Differential scanning calorimetry (DSC)

DSC experiments were performed on a Shimadzu DSC60. The equipment cell was calibrated with indium (mp 156.6 °C; $\Delta H_{fus} = 28.54 J/g$) and lead (mp 327.5 °C). Aluminum pans, containing approximately 1 mg of sample, were used under a dynamic N_2 atmosphere (50 mL/min) and a heating rate of 10 °C/min in the temperature range between 25 and 300 °C. As form III showed different thermal behavior, an isothermal experiment was conducted at 175 °C for periods of 15, 30, and 45 min.

2.3. Fourier transformed infrared spectroscopy (FTIR)

All experiments were conducted on a Perking Elmer IR spectrometer, with samples measured in KBr pressed pellets in the wavenumber range between 400 and 3400 cm^{-1} at room temperature, with a resolution of 4 cm^{-1}.

2.4. ^{1}H and ^{13}C-NMR analysis

Solution 1D and 2D NMR experiments (^{1}H, ^{13}C, DEPT-135, HSQC, and HMBC) spectra were performed by using a Bruker Avance DRX 400 spectrometer in DMSO-d_6 (deutered dimethyl sulfoxide, up to 99.9%) solution at 300 K, which was used as an internal standard (^{1}H: δ = 2.50 ppm; ^{13}C: δ = 39.50 ppm).

Solid-state ^{13}C-NMR (ssNMR) spectra were collected by using a Bruker Avance DRX 400 (9.4T) running at rotation of 10 kHz with cross polarization and using glycine (C=O: δ = 176.03 ppm) as an internal standard.

2.5. UV spectrophotometry

Spectral scans were performed between the wavelengths of 200 and 400 nm on MLX samples dissolved at 10 μg/mL in ethanol by using a Shimadzu 1800 spectrophotometer. Ethanol was used as the blank sample to correct for the instrumental background. Origin software (version 9.1) was used to analyze the data.

All described analyses were conducted within the validity period of all samples.

2.6. Evaluation of the biological activity

2.6.1. Animals

The anti-inflammatory activity was evaluated through the use of the carrageenan-induced paw edema test. Female Swiss mice (25–30 g) with free access to food and water were used. The animals were kept in a room with a 12 h light/dark cycle for a minimum of 3 days prior to the experiment, to allow acclimatization. The room temperature was maintained at 27 °C, which corresponds to the thermoneutral zone for mice [11]. This study was approved by the Ethics Committee on Animal Experimentation of the Federal University of Minas Gerais (Protocol 233/2016) and conducted in accordance with the S7A guide of the International Conference on Harmonization [12].

2.6.2. Paw edema induced by carrageenan

To measure paw volume, a plethysmometer (Model 7140, Ugo Basile, Italy) was used. The basal volume of the right hind paw was measured before the administration of any drug. Next, the animals were divided into the experimental groups in such a way that the mean volumes of each groups was similar. Carrageenan (400 μg/ 20 μL) was injected via the intraplantar (i.pl.) route. The vehicle (carboxymethylcellulose; CMC 1%), meloxicam A 15 mg/kg, meloxicam B 15 mg/kg, meloxicam A 30 mg/kg, meloxicam B 30 mg/ kg, or dexamethasone (10 mg/kg; positive control) were administered per os (p.o.) 30 min prior to the carrageenan injection. The volume of p.o. administration was 10 mL/kg. The paw volume of each animal was again measured at 2, 4, and 6 h after injection of the inflammatory stimulus. The results are expressed as the change in paw volume (μL) relative to the basal values [13].

2.6.3. Statistical analysis

The results are presented as the mean ± standard error mean (S.E.M.). Two-way ANOVA followed by Bonferroni's post hoc test was used to analyze paw volumes differences, with *P* values of < 0.05 considered significant. Statistical analyses were performed by using GraphPrism 5.0 (San Diego, USA) for Windows.

3. Results and discussion

As the samples from A and C showed identical X-ray diffraction patterns (form I; Fig. 2), we considered them to be the same material. Therefore, all other chemical and biological analyses were performed with samples from A (form I) and B (indicated by XRD as a mixture of some of form I and predominantly form III). The significant differences in peak positions and observed reflection planes, shown in Fig. 2, confirmed that there were two different polymorphs of the same material.

Thermal analysis was performed on separate aliquots. The DSC curves of samples from A and B are shown in Fig. 3. In the curve of the sample from pharmacy B, there is an incipient exothermal peak (4.47 J/g), at 206.6 °C. This peak was suggestive of crystallization or crystal transition, and was not present in the sample from pharmacy A (form I). After the melting point at approximately 260.0 °C, in both samples, similar behavior was observed.

Based on the observed thermal behavior, an isotherm at 175.0 °C, just below the beginning of the broad large transition peak, was analyzed to check the crystal transition observed at 206.6 °C. The XRD patterns shown in Fig. 4 were obtained after the isotherm, under tightly temperature control, after 15, 30, and 45 min. In all three distinct aliquots, we confirmed the occurrence of one phase transition. After 15 min, we observed the beginning of the conversion; after 45 min, the phenomenon was completed (Fig. 4).
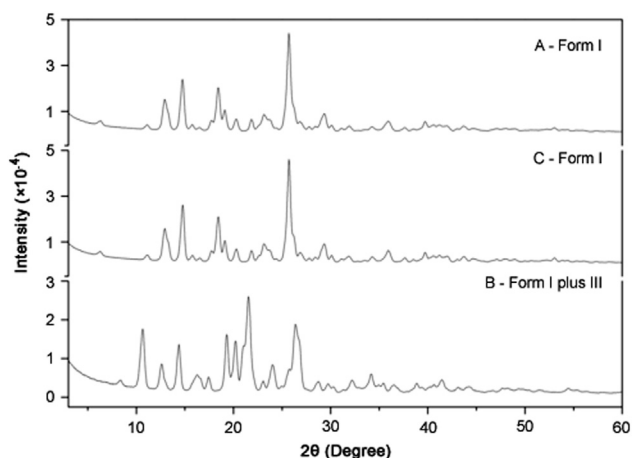
Fig. 2. X-ray diffraction patterns of samples from compounding pharmacies A, B, and C.
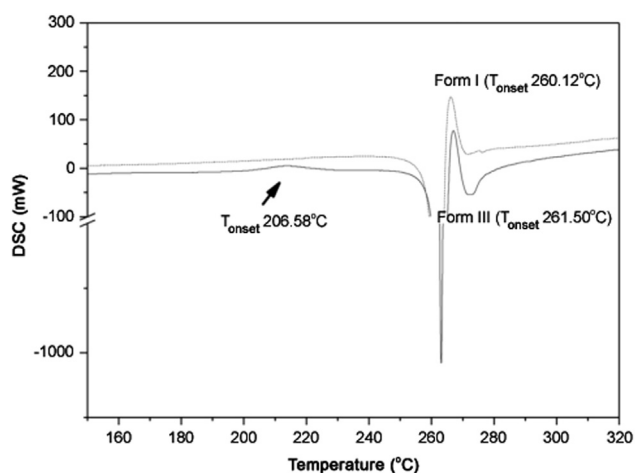

Fig. 3. DSC curves of samples from compounding pharmacies A and B superimposed, showing the presence of a small exothermic peak in the B sample. The y axis is broken for better visualization.
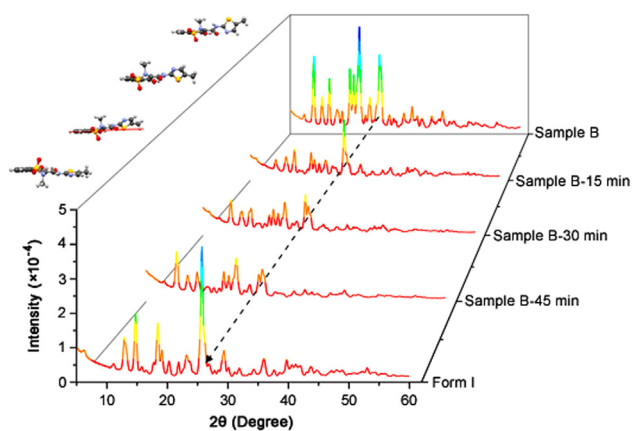

Fig. 4. Powder X-ray diffraction of compounding pharmacy B isotherm at 175 °C. The structures were fitted by using the Rietveld algorithm. The quotes indicate the sample from compounding pharmacy B, heated at 175 °C for 15, 30, and 45 min and the final product of the isotherm experiment (form I).

Through the comparison of the FTIR spectra from the samples from pharmacies A and B (Fig. 5), the absorptions were assigned to distinct peaks for each chemical functional group within the structure. The observed and assigned changes in the functional groups occurred at 1184–1176 cm^{-1}, 1526–1520 cm^{-1}, and 1550–
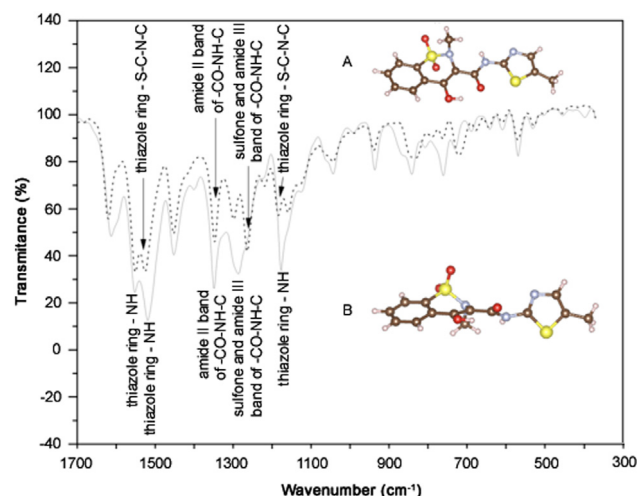

Fig. 5. Comparison of Fourier transform infrared spectra between form I and form III.

1552 cm^{-1} related to the stretching vibration of the thiazole ring, the asymmetric stretching vibration at 1264–1286 cm^{-1} of the sulfone, and amide III bands for the -CO-NH-C- group.

As observed in ssNMR (Fig. 6), C14 showed a double signal centered at 13.9 and 9.7 ppm for sample B; however, only one signal at 12.8 ppm was observed for sample A (form I; Fig. 6, Table 1).

The ^1H and ^{13}C-NMR spectra of meloxicam were collected in DMSO-d_6 (Supplementary material). After the material was solubilized in DMSO-d_6, all polymorphic characteristics were lost through the dissolution process. In solution, the NMR spectra were identical for both samples. Thus, the discussion of these results is valid for both samples.

The 1D and 2D NMR spectra (^1H, ^{13}C, DEPT-135, HSQC, and HMBC) were obtained under standard conditions (shown in Supplementary material). In the ^{13}C spectrum, the aromatic carbons C2, C3, C4, C5, C6, C7, and C16 resonated between 123.2 and 134.4 ppm, as expected. The methyl carbons C10 and C18 resonated at 37.9 and 11.7 ppm, respectively. The quaternary carbon C9 resonated at 114.2 ppm, whereas C8, which was connected to the OH group, resonated at 115.7 ppm. Finally, the carbonyl resonated at 168.4 ppm. These results were obtained through direct comparison with published data [4].

The solid-state ^{13}C-NMR spectra of the samples from compounding pharmacies A and B are shown in Fig. 6. All ^{13}C peaks were properly indexed and a higher number of carbon atoms for
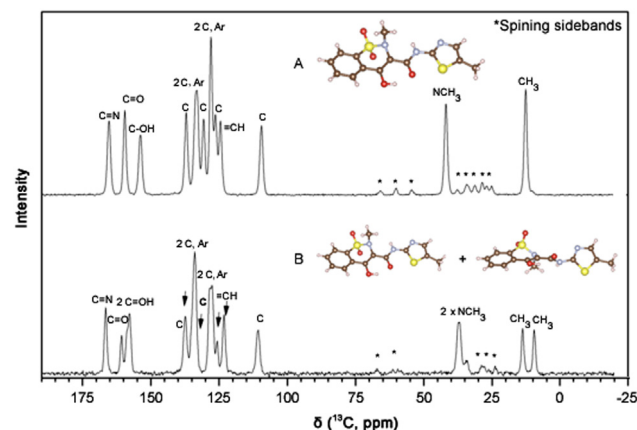

Fig. 6. ssNMR spectra for samples from compounding pharmacies A (form I) and B (form I plus form III).

Table 1
ssNMR assignment for ^{13}C signals.

Carbon	Chemical shift (δ, ppm)	
	Sample from A	Sample from B
C1	165.4	166.6
C2	159.6	160.8
C3	**153.9**	**157.9**
C4	137.1	137.4
C5	133.2	134.0
C6	133.2	134.0
C7	130.7	128.3
C8	130.7	128.3
C9	128.0	127.6
C10	126.4	125.8
C11	124.5	123.2
C12	109.5	110.7
C13	**42.0**	**37.0**
C14	**12.8**	**13.9 / 9.7**

sample from B was found compared with the expected spectrum. Through comparison with the spectrum of form I, this provided evidence of the existence of a mixture that contained some of form I and mainly form III (Table 1). This result was corroborated by the XRD measurements, which showed that form III was the major component of the mixture.

The UV analysis indicated common absorption maxima for forms I and III in ethanol solution at 205, 269 and 363 nm (Fig. 7). Special structural features may promote different solvation interactions that favor the appearance of tautomeric structures. This would be the case for forms I and III in water owing to the observed turn in the thiazole ring. However, the UV measurement conditions eliminate this possibility, as in standard literature procedures, the UV spectral measurement is obtained in ethanol, for solubility reasons. The contribution of each functional group to the absorption spectra of forms I and III is shown in Fig. 7.

In the UV spectra, a bathochromic shift from 215 nm to 219 nm and a hypsochromic displacement from 297 nm to 278 nm were observed. The Hirshfeld surface was calculated with the projection of the electrostatic potential highlighted by Spackman and Jayatilaka [14], Bojarska and Maniukiewicz [15], which allowed the complete assignment of UV spectra for both forms, I and III, respectively, in ethanol solution. There is a higher probability of interactions between the aromatic rings in form III, which favors the $\pi \rightarrow \pi^*$ transitions. The hydrogen on the OH group at C3 remains at a distance of approximately 1.69 Å in form I. In form III, the interaction is partial, mainly owing to the difficulties imposed by the increased distance to the same groups and atoms, now
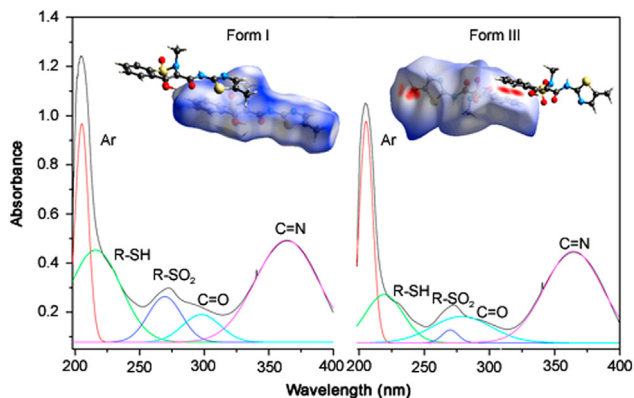
approximately 1.88 Å. This longer distance interaction justifies the hypsochromic displacement, as it requires higher energy to occur.

The carrageenan injection induced a marked and long-lasting paw edema that was already evident at 2 h after injection. Dexamethasone 10 mg/kg resulted in the strongest anti-edematogenic effect ($P < 0.001$), as expected, because it is a steroidal anti-inflammatory agent that acts in the early stages of the inflammatory process; this drug is often used as a positive control in comparative studies [16–19]. Nevertheless, owing to the side effects observed in the medicinal uses of this class of materials, it is necessary to obtain effective drugs that result in fewer adverse events. At present, the oxicams play an important role as anti-inflammatory agents [19,20].

Another hypothesis from the results of the biological evaluation for a sample B refers to its identity. As the analyses by XRD and ssNMR indicated the presence of a certain amount of polymorph I in a mixture with polymorph III in the sample from the compounding pharmacy B, the anti-edematogenic effect may be associated with the amount. This result shows the importance of the study of the biological activity of different polymorphs in drugs usually present in raw materials of pharmaceutical interest, both mistral or industrial, as well as for proper characterization in quality control steps [9,10].

Both meloxicam samples (from pharmacies A and B) reduced paw edema when administered 30 min before carrageenan. Meloxicam from pharmacy A (15 mg/kg) reduced paw edema at 4 h ($P < 0.001$) and 6 h ($P < 0.001$). The highest dose of meloxicam from pharmacy A (30 mg/kg) reduced paw edema at 2 h ($P < 0.01$), 4 h ($P < 0.001$) and 6 h ($P < 0.001$). Meloxicam from pharmacy B was not as effective as meloxicam from pharmacy A. Both doses of meloxicam from pharmacy B (15 and 30 mg/kg) reduced paw edema, but only at 4 h ($P < 0.001$). The differences between the two samples were more pronounced at the highest dose at 4 h ($P < 0.001$) and 6 h ($P < 0.01$) after the injection of carrageenan (Fig. 8).

To study the effects of the two meloxicam samples on the carrageenan-induced paw edema, the positive control of dexamethasone 10 mg/kg, which is frequently used in preclinical assays [16–19], was used, and resulted in the highest anti-edematogenic activity, as expected. This steroidal anti-inflammatory drug markedly inhibits the early stages of the inflammatory process, but may also induce many side effects. Thus, there is an ongoing search for other anti-inflammatory drugs with a safer profile and oxicams appear to be good candidates [20,21].
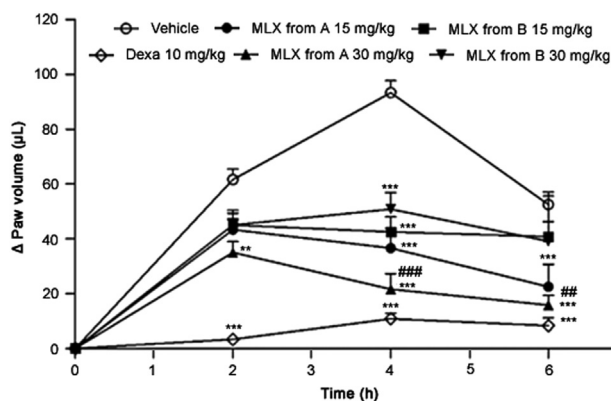

Fig. 8. Effect of meloxicam (MLX) from A and B compounding pharmacies (15 and 30 mg/kg, p.o.) or dexamethasone (Dexa; 10 mg/kg, p.o.) administered 30 min prior to the induction of the paw edema by i.pl. injection of carrageenan (Cg, 400 µg/paw). Each point represents the mean ± S.E.M. of six animals. ** and *** indicate significantly differences from the vehicle ($P < 0.01$ and $P < 0.001$, respectively). ## and ### indicate significantly difference from meloxicam B 30 mg/kg ($P < 0.01$ and $P < 0.001$, respectively).

Fig. 7. Total UV-spectra assignments of forms I and III associated with surface potentials obtained from the Hirshfeld surface analysis.

The i.pl. injection of carrageenan induced an acute and marked inflammatory response, characterized mainly by edema formation. This acute response most likely resulted from neutrophil migration and activation and also from the production of a variety of inflammatory mediators that induce vasodilation and increase vascular permeability [22,23]. In the present study, pre-treatment with both meloxicam samples reduced carrageenan-induced paw edema in mice. Others investigators have demonstrated the anti-inflammatory and analgesic activities of meloxicam in preclinical assays. These effects may result from reduced leukocyte migration and the reduced production of inflammatory mediators, as it has been shown that meloxicam attenuated the activation of nuclear factor-κB, inhibited COX-2 expression, and increased IL-10 production [24–26].

Meloxican form I was isolated from commercial samples from compounding pharmacies A and C. The sample from compounding pharmacy B, a mixture of forms I and III, was directly identified through the comparison of the X-ray diffraction patterns in patent US 20030109701 A1, [4]. Therefore, the sample from B was convoluted by the respective counterparts. Their Bragg reflections were independently indexed and extracted by the Pawley method. Once isolated and treated as one mixture, the crystallographic information for form III was extracted and used in order to obtain the Hirshfeld surface analysis for this polymorph alone (Fig. 9).

The Hirshfeld surface analysis assigns intermolecular interactions inside the unit cell packing. The analysis helps to understand the differences that were observed in the biological evaluation between samples from A (form I) and from the mixture in B (form I plus form III). The atomic distribution of form I, as shown in Fig. 9, contributes 89% of the overall interaction's distances (de × di) to

the potential surface, starting from as low as 1.2 Å up to 2.4 Å (Fig. 9; form I). All expected interactions are π…π, between 5-(thiazole) and 6-membered rings and N-H…S=O internally. In contrast, the overall interactions calculated for form III, were present in (de × di), as low as 1.0 Å and rose to over 2.8 Å (Fig. 9; form III) [14–26]. The observed turn around the thiazole ring in polymorph III increased the amount of interactions that contributed to different dissolution behavior. These observations not only explained the double signal of C14, but corroborated the increased intermolecular interactions seen for form III. From this data, we inferred that the intramolecular forces occurring at lower and also at higher distance in form III promoted stronger intermolecular interactions within and between the molecules inside the unit cell arrangement. This effect will result in a lower solubility (higher interactions inside the unit cell), as experimentally observed. In agreement with the observed behavior, meloxican was classified as class II in the Biopharmaceutical Classification System [27,28].

Through those observations, we related the results of the biological evaluation found for sample B (form I plus form III, lower activity), with adverse pharmacokinetic parameters, such as bioabsorption and distribution. As form III presents intramolecular interactions at a lower distance (1.0 Å) in addition to higher distances (over 2.8 Å), when compared with the same parameters for pure form I, the internal cell packing forces will be increased, which results in a more difficult solubilization process. The Hirshfeld surface analysis showed C14 close to S in the thiazole ring on one side and to the hydroxyl group in the six-membered ring in the middle of the structure. For form I, only the hydroxyl group interaction was observed, which explained the ssNMR single signal for C14. In this case, a reduction of the amount of
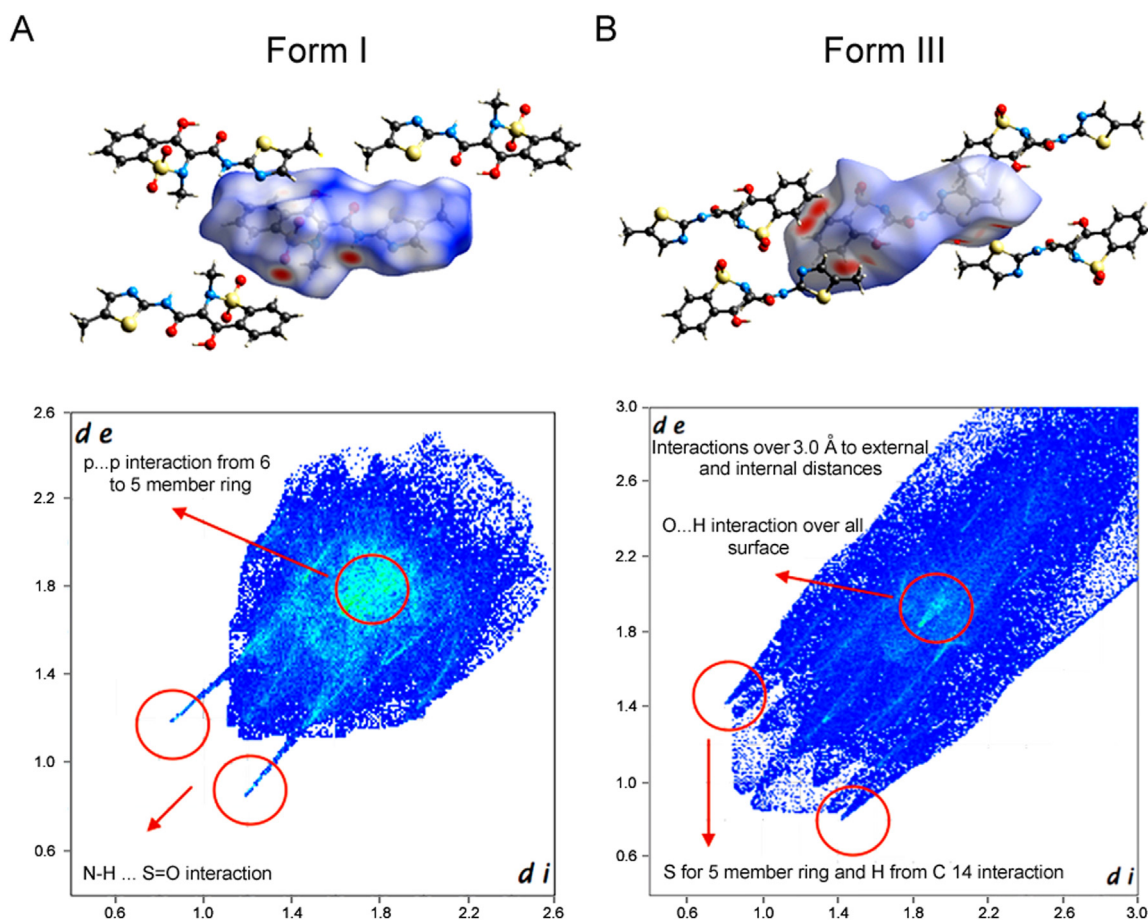

Fig. 9. Fingerprint plots: intermolecular interactions within the samples from compounding pharmacies A and B that show the total Hirshfeld surface area.

solubilized form III in comparison with form I, over the same so-lubilization time, will affect the available drug amount after ad-ministration differently for both forms.

4. Conclusion

X-ray diffraction, DSC, and ssNMR analysis indicated the pre-sence of two polymorphs of meloxicam, forms I and III, in the sample from pharmacy B, freely sold in compounding pharmacies from which the samples were acquired.

The biological test indicated a lower degree of anti-edema ac-tivity for the polymorph III when present as major component in the sample from compounding pharmacy B, which also contained form I in the mixture. The Hirshfeld surface analysis of forms I and III provided an explanation of the solubility difference, which was experimentally observed for both compounds; form III is less so-luble than form I.

Although less active, form III is a major component freely sold in compounding pharmacy B, which justified the difference in biolo-gical activity between the sample from compounding pharmacy A (form I) and the sample from pharmacy B (form I plus III) observed during the paw edema test conducted in female Swiss mice.

Our results highlighted the need for full crystallographic char-acterization and separation of freely used raw material in com-pounding pharmacies as an indispensable quality control protocol to ensure the desired drug dose/effect. The main concern over the lack of an adequate quality control was demonstrated to be unexpected dif-ferences in biological activity that could compromise human health.

Conflicts of interest

The authors declare that there are no conflicts of interest.

Acknowledgments

Appendix A. Supplementary material

Supplementary data associated with this article can be found in the online version at http://dx.doi.org/10.1016/j.jpha.2017.12.006.

References

[1] I.I. Roberts, J.D. Morrow in: J.G. Hardman, L.E. Limbird, Goodman & Gilman's the pharmacological basis of therapeutics, McGraw-Hill, New York, 2001:713–714.

[2] British Pharmacopoeia Commission, British Pharmacopoeia, Medicines & Healthcare products Regulatory Agency, TSO, London, 2013.

[3] The United States Pharmacopoeia, third fourth ed., United States Pharmaco-peial Convention, Rockville:3403–3405, 2011.

[4] L. Coppi, M.B. Sanmarti, M.C. Clavo, Crystalline forms of meloxicam and pro-cesses for their preparation and interconversion. Patent US 20030109701 A1, 2003.

[5] P. Luger, K. Daneck, W. Engel, et al., Structure and physicochemical properties of meloxicam, a new NSAID, Eur. J. Pharm. Sci. 4 (1996) 175–187.

[6] A. Burger, R. Ramberger, On the polymorphism of pharmaceuticals and other molecular crystals. I, Microchim. Acta 72 (1979) 259–271.

[7] A. Burger, R. Ramberger, On the polymorphism of pharmaceuticals and other molecular crystals. II, Microchim. Acta 72 (1979) 273–316.

[8] J. Haleblian, W. McCrone, Pharmaceutical applications of polymorphism, Pharm. Sci. 58 (1969) 911–929.

[9] E.H. Lee, A practical guide to pharmaceutical polymorph screening & selection, Asian J. Pharm. Sci. 9 (I4) (2014) 163–175.

[10] M. Descamps, J.F. Willart, Perspectives on the amorphisation/milling re-lationship in pharmaceutical materials, Adv. Drug Deliv. Rev. 100 (2016) 51–66.

[11] C.J. Gordon, Thermal biology of the laboratory rat, Physiol. Behav. 47 (1990) 963–991.

[12] International Conference on Harmonization, Safety pharmacology studies for human pharmaceuticals (S7A), 2000: 13.

[13] S.H. Ferreira, A new method for measuring variations of rat paw volume, J. Pharm. Pharmacol. 31 (1979) 648.

[14] M.A. Spackman, D. Jayatilaka, Hirshfeld surface analysis, CrystEngComm 11 (2009) 19–32.

[15] J. Bojarska, W.J. Maniukiewicz, Investigation of intermolecular interactions in finasteride drug crystals in view of X-ray and Hirshfeld surface analysis, Mol. Struct. 1099 (2015) 419–426.

[16] H.J. Koo, K.H. Lim, H.J. Jung, et al., Anti-inflammatory evaluation of gardenia extract, geniposide and genipin, J. Ethnopharmacol. 103 (2006) 496–500.

[17] M. Fezai, L. Senovilla, M. Jemaà, et al., Analgesic, anti-inflammatory and anticancer activities of extra virgin olive oil, J. Lipids 2013 (2013) 1–7.

[18] D.G. Soares, A.M. Godin, R.R. Menezes, et al., Anti-inflammatory and antinociceptive activities of azadirachtin in mice, Planta Med. 80 (2014) 630–636.

[19] T. Göncü, E. Oğuz, H. Sezen, et al., Anti-inflammatory effect of lycopene on endotoxin-induced uveitis in rats, Arq. Bras. Oftalmol. 79 (2016) 357–362.

[20] H. Schäcke, W.-D. Döcke, K. Asadullah, Mechanisms involved in the side effects of glucocorticoids, Pharmacol. Ther. 96 (2002) 23–43.

[21] S. Xu, C.A. Rouzer, L.J. Marnett, Oxicams, a class of nonsteroidal anti-in-flammatory drugs and beyond, IUBMB Life 66 (2014) 803–811.

[22] D.A.R. Valério, T.M. Cunha, N.S. Arakawa, et al., Anti inflammatory and an-algesic effects of the sesquiterpene lactone budlein A in mice: inhibition of cytokine production-dependent mechanism, Eur. J. Pharmacol. 562 (2007) 155–163.

[23] A.C. Rocha, E.S. Fernandes, N.L. Quintão, et al., Relevance of tumour necrosis factor-α for the inflammatory and nociceptive responses evoked by carra-geenan in the mouse paw, J. Pharmacol. 148 (2006) 688–695.

[24] G. Engelhardt, D. Homma, K. Schlegel, et al., Anti-inflammatory, analgesic, antipyretic and related properties of meloxicam, a new non-steroidal anti-inflammatory agent with favourable gastrointestinal tolerance, Inflamm. Res. 44 (1995) 423–433.

[25] G. Engelhardt, Pharmacology of meloxicam, a new non-steroidal anti-in-flammatory drug with an improved safety profile through preferential in-hibition of COX-2, Br. J. Rheumatol. 35 (1996) 4–12.

[26] N.A. El-Shitany, E.A. El-Bastawissy, K. El-desoky, Ellagic acid protects against carrageenan-induced acute inflammation through inhibition of nuclear factor kappa B, inducible cyclooxygenase and proinflammatory cytokines and en-hancement of interleukin-10 via an antioxidant mechanism, Int. Im-munopharmacol. 19 (2014) 290–299.

[27] F.P.A. Fabbiani, L.T. Byrne, J.J. McKinnon, et al., Solvent inclusion in the struc-tural voids of form II carbamazepine: single-crystal X-ray diffraction, NMR spectroscopy and Hirshfeld surface analysis, CrystEngComm 9 (2007) 728–731.

[28] D.R. Weyna, M.L. Cheney, N. Shan, et al., Improving solubility and pharma-cokinetics of meloxicam via multiple-component crystal formation, Mol. Pharm. 9 (2012) 2094–2102.